World Academy of Science, Engineering and Technology
International Journal of Structural and Construction Engineering
Vol:17, No:2, 2023

# Data Compression in Ultrasonic Network Communication via Sparse Signal Processing

Beata Zima, Octavio A. Márquez Reyes, Masoud Mohammadgholiha, Jochen Moll, Luca De Marchi



***Abstract*—**This document presents the approach of using compressed sensing in signal encoding and information transferring within a guided wave sensor network, comprised of specially designed frequency steerable acoustic transducers (FSATs). Wave propagation in a damaged plate was simulated using commercial FEM-based software COMSOL. Guided waves were excited by means of FSATs, characterized by the special shape of its electrodes, and modeled using PIC255 piezoelectric material. The special shape of the FSAT, allows for focusing wave energy in a certain direction, accordingly to the frequency components of its actuation signal, which makes a larger monitored area available. The process begins when a FSAT detects and records reflection from damage in the structure, this signal is then encoded and prepared for transmission, using a combined approach, based on Compressed Sensing Matching Pursuit and Quadrature Amplitude Modulation (QAM). After codification of the signal is in binary, the information is transmitted between the nodes in the network. The message reaches the last node, where it is finally decoded and processed, to be used for damage detection and localization purposes. The main aim of the investigation is to determine the location of detected damage using reconstructed signals. The study demonstrates that the special steerable capabilities of FSATs, not only facilitate the detection of damage but also permit transmitting the damage information to a chosen area in a specific direction of the investigated structure.

***Keywords*—**Data compression, ultrasonic communication, guided waves, FEM analysis.

## I. Introduction

ULTRASONIC guided waves have been efficiently used in structural health monitoring applications [1]. They are sensitive to various defect types like cracks [2], [3], impact damages [4] or debonding [5] which makes them an attractive tool for diagnostics purposes. Special attention was paid to wave-based diagnostics of thin-walled structures [6]-[8], which are common components of machines, buildings, or ships. The idea of using guided waves in damage detection in plate-like structures is based on registering signals by sensors located on the plate surface. The registered data are further processed to extract the information about detected damage and correctly interpret its content. As mentioned, the damage detection procedure is mainly given by a simple and inexpensive technical implementation, based on a distributed array of transducers. The inherent capability of these transducers to share information between the network nodes, together with the waves capability of monitoring relatively large areas without significant energy loss, might be used in the next generation of intelligent Structural Health Monitoring (SHM) systems [9]. Wave-based acoustic communication is an attractive and less expensive alternative to cable-based systems or radio-frequency communication. Therefore, in recent years the interest in developing robust digital communication methods has grown significantly [10], [11]. One of the greatest challenges in this field is to reduce the amount the data required to transfer information between nodes, without losing information in the process. A very advantageous situation arises by encoding an entire signal using well-defined parameters, thereby providing a new signal whose amount of data is much smaller than the number of measurements present in the original signal, e.g. only 10%. Then, by using these parameters at the base station, the message would be decoded, processed and interpreted for further diagnostics. The idea of ultrasonic communication has been presented in many previous papers [10], [11] but the algorithm presented in this study allows to transfer enough information to reconstruct the entire signal, and not only the results of the pre-processing.

Beata Zima is with Gdansk University of Technology, Poland (e-mail: beata.zima@pg.edu.pl).

## II. Algorithm of Ultrasonic Network Communication

This section contains the description of the developed algorithm for signal compression and ultrasonic communication employed in the study.

### A. Signal Compression

The main idea of the developed algorithm is based on the assumption that each signal can be uniquely defined by several parameters, which can be encoded and decoded in a base station. In this study, the iterative signal reconstruction has been performed by compressed sampling matching pursuit algorithm (CoSaMP) [12], which offers rigorous bounds on computational cost and storage, because the amount of encoding parameters is significantly smaller than the number of measurements in the original signal. Furthermore, the number of required parameters is also much smaller than those presented by the Nyquist-Shannon sampling theorem. The number of samples $m$ needed to ensure that the sampling map embeds the set of $s$-sparse signals is equal to:

$$m = O\left(s \log(N/s)\right) \tag{1}$$

where $N$ denotes the number of measurements in the input signal. In the presented case the minimal number of samples required for accurate signal reconstruction was equal to 10%, which significantly facilitates information transfer, these

samples have to be chosen randomly. The exemplary signal with chosen samples marked is presented in Fig. 1.

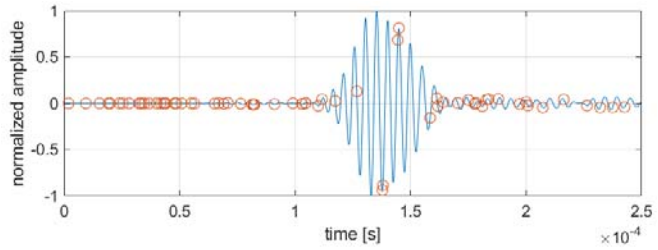


Fig. 1 Exemplary time domain wave propagation signal with selected samples marked

### B. Encoding the Information

The next step is to encode the information representing the selected samples. Each sample is uniquely defined by the amplitude $A$ and the registration time $T$. Because one of the challenges is to encode the signal using the smallest amount of data possible, both the amplitude and registration time are encoded in one number. To this aim, the amplitude and the time can be considered as the *coordinates* in 2D space. Let us imagine that the signal can be plotted on a grid (Fig. 2). The grid size is defined by the time step $dt$ (horizontal direction) and the parameter $S$ (vertical direction). The value of $S$ is arbitrarily defined by the investigator. It must be mentioned that the high value of $S$ results in a smaller amount of information that has to be transferred, however, the accuracy of the signal reconstruction is also lower. The high value of $S$ results in high reconstruction accuracy but on the other hand, the process of information transfer is more difficult and time-consuming.

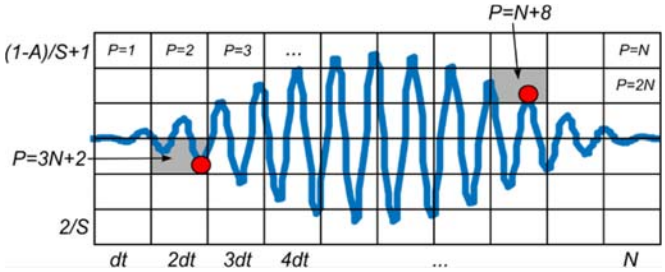


Fig. 2 The illustration of the encoding of the information about the amplitude and the registration time of selected samples

Each row contains $N$ elements, which is the number of measurements in the original signal. Because we take into account the normalized signals, the maximal amplitude is equal to 1, and the minimum amplitude is equal to -1. Therefore, each column contains $2/S$ elements. In the presented example in Fig. 2, the parameter $S$ is equal to 1/3, so the number of rows is equal to 6. As mentioned, the sample can be uniquely defined by the amplitude $A$ and the registration time $T$ but also by the number $P$ of the grid eye. Using the amplitude and registration time can be encoded in the following way:

$$P = \left\lfloor \frac{1-A}{S} \right\rfloor \cdot N + \frac{T}{dt} \tag{2}$$

where $A$ is the amplitude, $T$ is the registration time and $N$ is the number of measurements in the signal. The number $P$ is an integer and it can be rewritten in binary form which facilities further message transmission.

To codify the information, the QAM has been applied here. QAM is based on the modification of the amplitude and phase of the signal, while the carrier frequency is maintained the same throughout time. A representing binary stream is divided into symbols, while each symbol has uniquely assigned a string of ones and zeros. For example, if we want to use a symbol with 4 bits, our dictionary will contain $4^2 = 16$ symbols. Thus, QAM has different formats depending on the number of symbols (8-QAM, 16-QAM, 32-QAM, etc.). An 8-bit word 1110 0000 has been mapped in the constellation diagram presented in Fig. 3. The amplitude and the phase shift are assigned to the symbol $s(t)$ by the following expression:

$$s(t) = A'\cos\left(2\pi ft + \phi\right) = A'e^{(i2\pi ft+\phi)} \tag{3}$$

where $f$ is the carrier frequency.

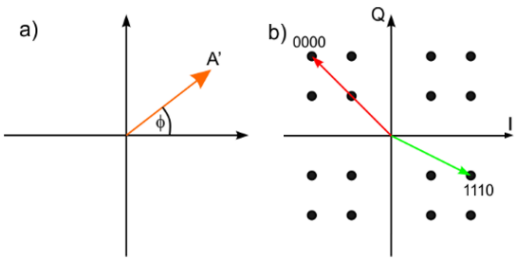


Fig. 3 (a) Phasor representation: each element can be described by the amplitude and phase shift, (b) digital 16-QAM with example constellation points

To define the excitation signal, we translate our message or stream of bits according to 16-QAM (for our particular case). The in-phase $I$ part of every symbol is mounted over the carrier signal, while the quadrature $Q$ part is multiplied by the same carrier frequency shifted 90°, these two signals are then mixed, generating a symbol signal to be transmitted. For instance, the digital message [1 1 1 0] presented in Fig. 3 (b), would be modulated in two signals ($I$ & $Q$) of different amplitude and shifted in phase, but with a single central frequency of 150 kHz, these are then summed together as presented in Fig. 4.

The sum of the signals is then modulated with a Hann window to avoid the excitation of unwanted frequencies and improve transmission.

### C. Information Transfer

The codified information has to be transferred between the network nodes. To this aim, the FSATs with unique directivity capabilities can be fruitfully used. The important advantage of the FSATs is the possibility to propagate the wave in a certain direction depending on the excitation frequency. To demonstrate the directivity capabilities the exemplary propagation pattern for a frequency of 200 kHz is presented in Fig. 5. The directivity capabilities of the FSATs are provided by the spiral shape of its electrodes. Because the wave energy

is focused in one direction, one can avoid the high-energy reflections from the boundaries, which may affect the registered signals and, in consequence, the transferred information. Moreover, focusing the energy permits sending information in a certain direction between network nodes with specified localizations.

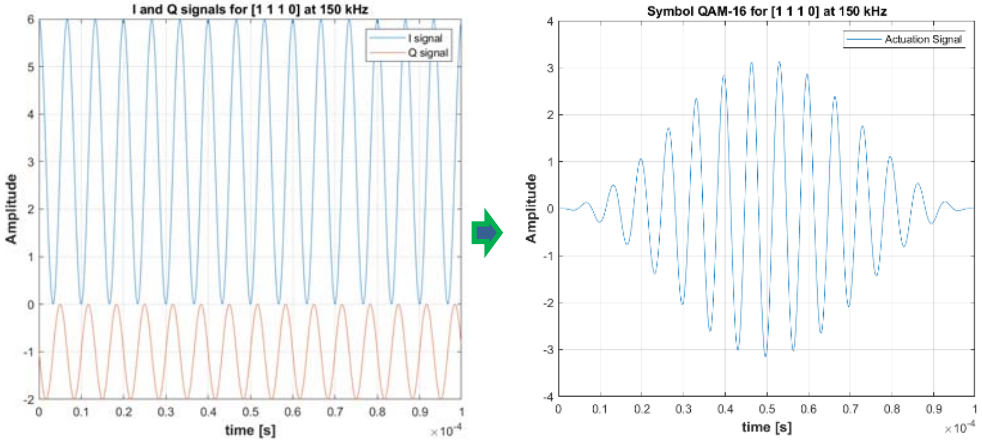


Fig. 4 In-phase (I) and Quadrature (Q) signals modulated and mixed to generate a symbol for [1 1 1 0] at 150 kHz

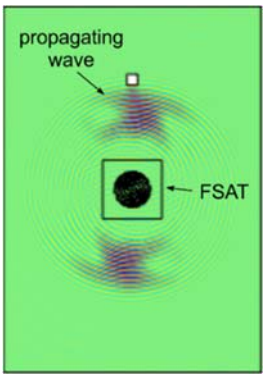


Fig. 5 Visualization of wave excited by the FSAT propagating in one direction

### *D. Decoding the Information*

The signal registered by the next FSAT must be decoded so in the first step the bit streams must be extracted. To do this, the opposite procedure or QAM demodulation process is to be applied. To extract the *I* and *Q* elements of the received signal, a local oscillator and phase shifter of 90° at reception is to be used: the product of the received signal with each of the phases of the local oscillator produces two new signals, which are then filtered to remove high-frequency components, from where we obtain the *I* and *Q* components. With these, we recreate the original constellation and/or our original bit stream. After rewriting the bit streams into decimal number *P*, the time *T* and the amplitude *A* can be calculated as:

$$A = 1 - \left( \left\lfloor \frac{P}{N} \right\rfloor + 1 \right) \cdot S \tag{4}$$

$$T = \left( P - N \left( \frac{1 - A}{S} - 1 \right) \right) \cdot dt \tag{5}$$

### *E. Signal Reconstruction*

In the last step the amplitudes *A* and registration times *T* are calculated, the signal is then reconstructed by using CoSaMP recovery algorithm and can be processed in the further steps of the diagnostic procedure.

## III. Numerical Simulations

To demonstrate the performances of the FSATs in damage detection as well as in ultrasonic communication, we have simulated a Lamb wave propagation in a 3D numerical model of an aluminum plate, characterized by the following parameters material: elastic modulus 70 GPa, Poisson's ratio 0.3 and material density 2700 kg/m$^3$ [13]. The dimensions of the considered plate were 500 mm x 500 mm, while the thickness was 1 mm. The FSAT was modeled as PIC255 piezoelectric material, with customized-shaped electrodes. This tailored-shaped transducer presents directional capabilities. The numerical simulations were performed with commercial FEM-based software COMSOL. For accurate modeling of ultrasonic guided waves propagation and the piezoelectric effect of the transducers, two physics modules have to be incorporated in this study: "Structural Mechanics" and "Electrostatics". The excitation was applied as time-dependent voltage in the form of an amplitude-modulated five-cycle sine function. The built-in low reflection boundary condition was used at the plate boundaries to minimize the influence of side reflections from plate edges.

To reduce the total simulation time, the numerical simulations were conducted in two stages. In the first one, the numerical simulation has been performed to model the wave reflection from damage in the form of cut-through plate thickness. For damage detection, the preferential frequency of 200 kHz has been employed. The geometry of the plate model together with the propagation pattern is presented in Fig. 6. The signal registered by the FSAT is presented in Fig. 7. For the sake of simplicity, the differential signal is taken into account

in the further steps. The reflection from the damage has been marked with a grey color. The differential signals are usually easier to compress and transfer because they contain the zero-amplitude part with no information about the structural state. Thus, it does not have to be encoded and reconstructed.

In the second stage, the encoded message was transferred by means of mechanical waves, propagating from the FSAT that registered the damage to a second one located 200 mm apart as shown in Fig. 8.

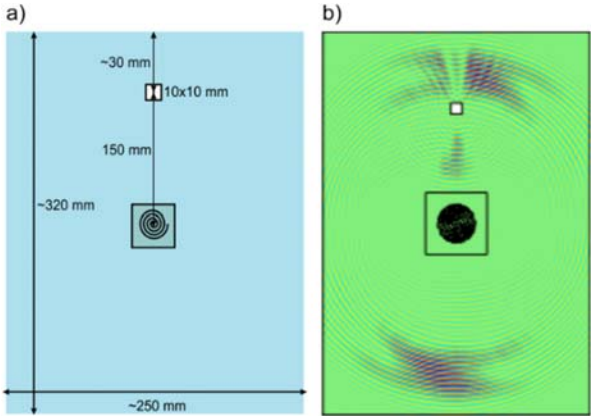


Fig. 6 Numerical simulations: (a) geometry of plate model, (b) wave reflection from damage

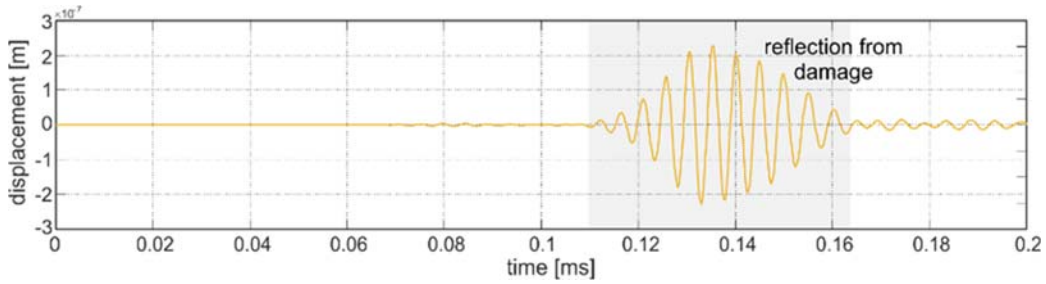


Fig. 7 Differential signal registered by the FSAT located in the middle point of the plate

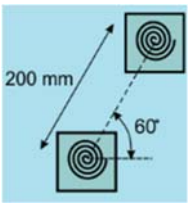


Fig. 8 Transducer network comprised of two FSATs at a distance of 200 mm

## IV. Results

### A. Signal Pre-processing

According to the above-described procedure, the samples essential to reconstruct the signal have been randomly chosen. Their number was equal to only 10% of the measurements in the original signal. Because this paper is mainly focused on presenting the concept of ultrasonic data communication, the information representing only two samples will be transferred between two network nodes. The chosen signal samples are indicated in blue color in Fig. 9.

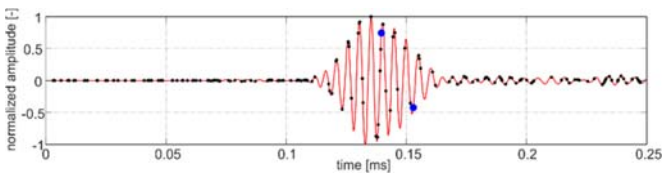


Fig. 9 Processed signal with chosen samples marked

In the following study, the parameter $S$ was defined as 0.0002. The amplitudes were $A1 = 0.744$ and $A2 = -0.426$ and their respective times of flight are equal to $T1 = 1.3965\times10^{-4}$ sec and $T2 = 1.529\times10^{-4}$ sec. The applied time step $dt$ was $1.505 \times 10^{-7}$ sec. and the established parameter $S$ was 0.0002. For such data, the values of $P1$ and $P2$ calculated according to (2) were equal to 1196409 and 6673969, which can be rewritten using a binary system:

- $P1$ = [0001 0010 0100 0001 0111 1001]
- $P2$ = [0110 0101 1101 0110 0011 0001].

### B. Signal Compression and Encoding

By using 16-QAM, each of the messages ($P1$ and $P2$) was codified in 6-symbol signals, one symbol per every 4 bits. In order to improve communication, an additional dummy symbol [0 0 0 0] was added at the beginning of every transmitted signal to indicate where transmission starts and supports signal synchronization at reception. Additionally, for the sake of simulation time and resources, we divided each message into 2, providing a total of 4 signals of 4 symbols each as presented in Fig. 10.

### C. Message Transferred between the Nodes

In the next step, the excitation signals were applied to the FSAT localized near the center of the plate. Because the excitation frequency was 150 kHz, the message was directed to the second FSAT located at 200 mm and 60° with respect to the first (transmission) FSAT as depicted in Fig. 11.

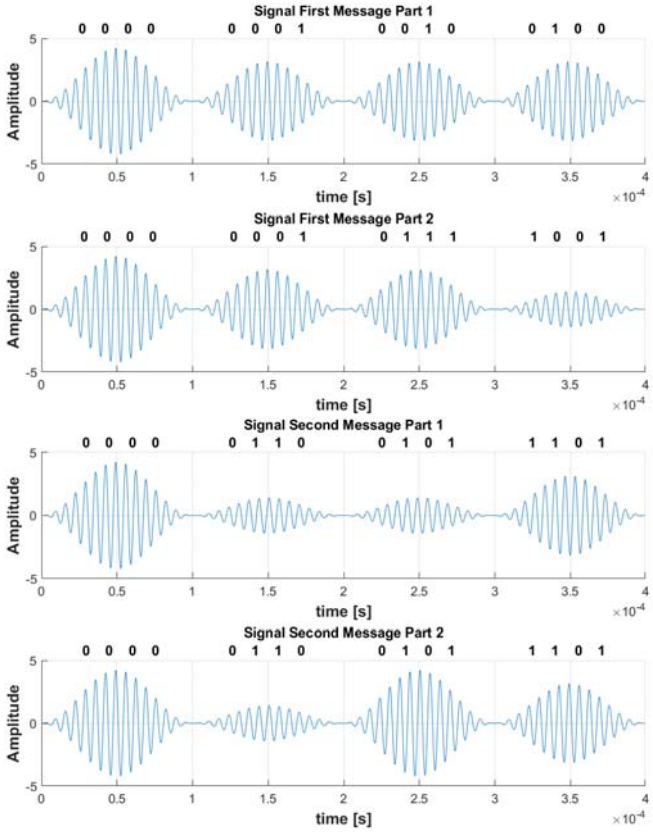


Fig. 10 Two messages of 32-bit streams modulated using 16-QAM into 4 excitation signals of 3 symbols with additional dummy start symbol [0 0 0 0]

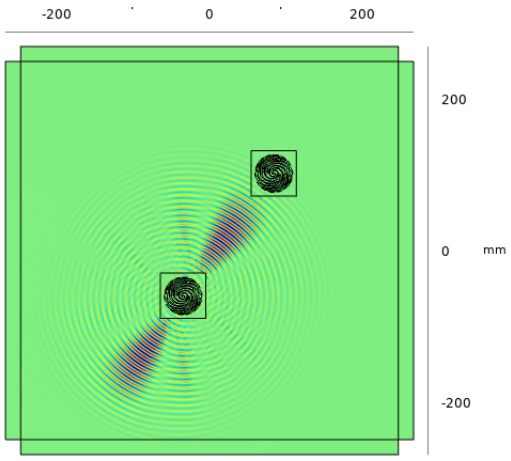


Fig. 11 Visualization of acoustic communication between two FSATs: The message is modulated over a 150 kHz frequency carrier signal so the transmitter FSAT propagates the message in direction of a second, reception, FSAT

### *D. Decoding the Message and Signal Reconstruction*

After simulation, we extracted the signal recorded by the reception FSAT (Fig. 11). In Fig. 12 is displayed an example of one of the actuation signals and its respective reception registered by the receiver FSAT after crossing the acoustic medium.

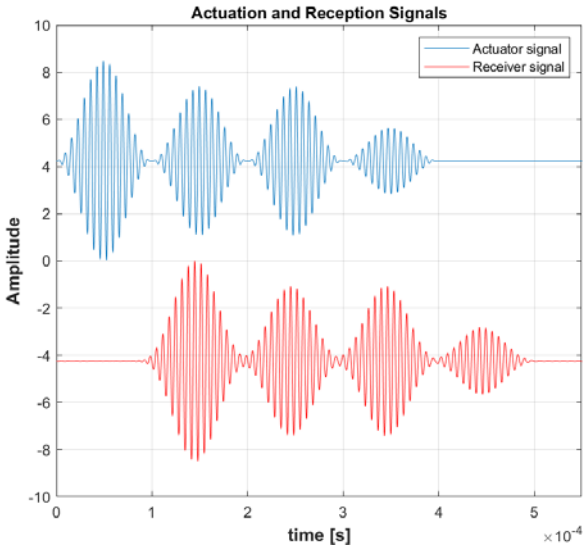


Fig. 12 Actuation signal applied to the transmitter FSAT in blue and the received signal registered by a second FSAT located 200 mm apart in red

The signals registered by the reception FSAT are demodulated according to the procedure described in Section II *D*, from where the first element, the dummy symbols are removed from the two sections of each message. The two parts of each message are then combined to draw (Fig. 13) the respective constellation diagram for each received message.

From the constellation diagram for the first message of Fig. 13, we can see the acquired 6 symbols representing the digital message: [0001 0010 0100 0001 0111 1001]. The bit order is defined by the order of the incoming symbols. From the same figure (Fig. 13) we can also verify the received bit stream divided into six symbols, representing the second message: [0110 0101 1101 0110 0011 0001]. Although there is an identifiable bias from the originally transmitted signals and the received ones in Fig. 13, it is too small to represent any inter-symbol interference and the message does not present any ambiguity for 16-QAM. The previous is given from the idealized environment of the FEA simulation, in an experimental application, it is expected that signals captured by the reception FSAT would content high channel noise and even additional modes that were traveling across the medium. This would present difficulties in message reception, recovery and interpretation. As we can see, the decoded messages correspond to the sent messages *P1* and *P2*. This proved that the proposed approach based on QAM is suitable for ultrasonic communication.

The procedure described above should be repeated for all samples required for correct signal reconstruction. For clarity, we presented the transfer of only two messages between the FSAT network. After transferring and decoding the data for all samples, the signal can be reconstructed using CoSaMP. The final result in the form of the reconstructed signal is given in Fig. 14. The reconstructed signal coincides well with the original signal and the reflection from the defect is clearly visible.

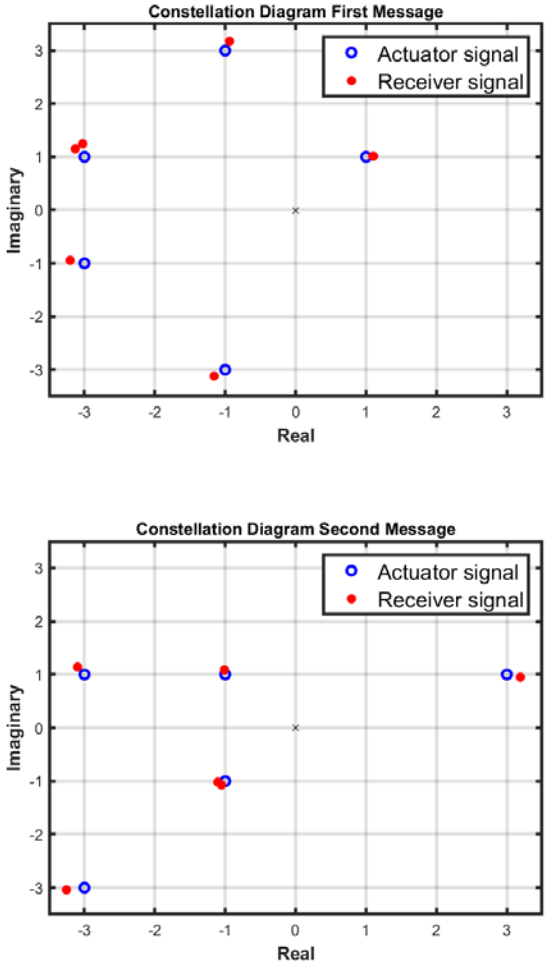


Fig. 13 Two constellation diagrams for transmitted messages comprised of 6 symbols each: The constellations of the original messages are plotted in blue, while the demodulated received signals after simulation are colored in red

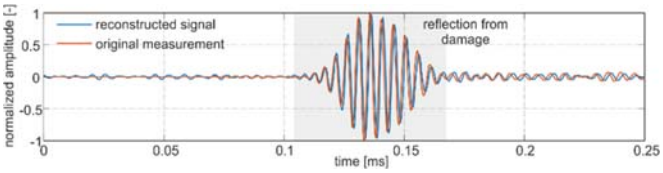


Fig. 14 The comparison of the original and reconstructed signal

### *E. Signal Processing*

The last stage is focused on the processing of the reconstructed signal. The reflection registered in the signal has been indicated and identified as a reflection from the damage. The time of flight of an additional wave packet has been determined using the cross-correlation method and in this study, it was equal to 0.1208 ms. By solving the well-known Lamb-Rayleigh dispersion equation [14] for an aluminum plate considered in numerical studies, the group velocity for an excitation frequency of 200 kHz was determined as 2298 m/s. Based on the time of flight and the velocity the distance between the FSAT, the damage can be estimated: it is equal to 0.138 m. Because of the directivity capability of the FSAT, the frequency of 200 kHz is associated with the vertical direction of the main lobe. If the distance and the direction of the main lobe is known, the detected damage might be localized (Fig. 15).

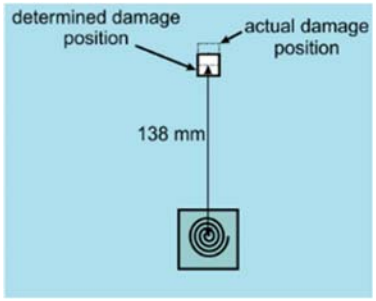


Fig. 15 Results of damage detection and localization

## V. Conclusion

This article presents the results provided by FEM analysis concerning data compression in ultrasonic network communication. It was demonstrated that the novel transducers with directivity capabilities can be used in damage detection procedures as well as communication nodes in the next generation of SHM systems. The study proved that the information about the signal can be successfully transferred and decoded in the last node and further used in damage detection and localization applications. The compressed sensing-based approach allowed for using a significantly smaller amount of data than contained in the original signal which facilitated message transfer.

## Acknowledgment

BZ gratefully acknowledges the support of the Foundation for Polish Science (FNP). OMR and JM gratefully acknowledge financial support by the German Research Foundation (DFG) under grant 349435502. MM and LDM gratefully acknowledge funding from the European Union's Horizon 2020 project Guided Waves for Structural Health Monitoring (GW4SHM, GA: 860104).

## References

[1] M. Mitra, and S. Gopalakrishnan, "Guided wave based structural health monitoring: A review," *Smart Mater. Struct.*, vol. 25(5), pp. 053001–053027, 2016.

[2] P. Kudela, M. Radzienski, W. Ostachowicz, and Z. Yang, ''Structural health monitoring system based on a concept of Lamb wave focusing by the piezoelectric array,'' *Mech. Syst. Signal Process.*, vol. 108, pp. 21–32, 2018.

[3] J. Moll, L. De Marchi, C. Kexel, and A. Marzani, ''High resolution defect imaging in guided waves inspections by dispersion compensation and nonlinear data fusion,'' *Acta. Acust. Unitec. Ac.*, vol. 103, no. 6, pp. 941–949, Nov. 2017.

[4] P. Kudela, M. Radzienski, and W. Ostachowicz, ''Impact induced damage assessment by means of Lamb wave image processing,'' *Mech. Syst. Sig. Process.*, vol. 102, pp. 23–36, 2018.

[5] B. Zima, "Baseline-free debonding detection in reinforced concrete structures by elastic wave propagation," *Measurement*, vol. 172, pp. 108907, 2021.

[6] J. Moll, R.T Schulte., B. Hartmann, C.P. Fritzen., O. Nelles, "Multi-site damage localization in anisotropic plate-like structures using an active guided wave structural health monitoring system," *Smart Mater. Struct.*, vol. 19(4), 2010.

[7] L. De Marchi, A. Marzani, N. Speciale, E. Viola, „A passive monitoring

technique based on dispersion compensation to locate impacts in plate-like structures," *Smart Mater. Struct.*, vol. 20(3), 2011.

[8] B. Zima, "Damage detection in plates based on Lamb wavefront shape reconstruction," Measurement, vol. 177, pp. 109206–109228, 2021.

[9] S. Das, H. Salehi, Y. Shi, S. Chakrabartty, R. Burgueno, and S. Biswas, ''Towards packet-less ultrasonic sensor networks for energy-harvesting structures,'' *Comput. Commun*., vol. 101, pp. 94–105, 2017.

[10] F. Zonzini, L. D. Marchi, N. Testoni, C. Kexel, and J. Moll, ''Guided-wave MIMO communication on a composite panel for SHM applications,'' *Proc. SPIE Health Monitor. Struct. Biol. Syst.*, vol. 11381, 2020.

[11] O.A. Marquez Reyes, J.Moll, F. Zonzini, M. Mohammadgholiha, L. De Marchi, "Quadrature Amplitude Modulation for Acoustic Data Communication in Ultrasonic Structural Health Monitoring Systems," *Proc. of the 2021 48th Annual Review of Progress in Quantitative Nondestructive Evaluation. 2021*, July 28–30, 2021.

[12] D. Needell and J.A. Tropp, "CoSaMP: Iterative signal recovery from incomplete and inaccurate samples," *App. Comp. Harm. Anal*. vol 26(3), pp. 301-321, 2009.

[13] O.A. Marquez Reyes, B. Zima., J. Mol., M. Mohammadgholiha, L. De Marchi, "A Numerical Study on Baseline-Free Damage Detection Using Frequency Steerable Acoustic Transducers," *Lecture Notes in Civil Engineering, European Workshop on Structural Health Monitoring*, vol. 270, pp. 24-33, 2023.

[14] J.L. Rose, Ultrasonic Waves in Solid Media. Cambridge University Press, Cambridge, 2004.